# Cramér-Rao Bounds for UMTS-Based Passive Multistatic Radar

Sandeep Gogineni, *Member, IEEE*, Muralidhar Rangaswamy, *Fellow, IEEE*, Brian D. Rigling, *Senior Member, IEEE*, and Arye Nehorai, *Fellow, IEEE*

***Abstract*—Owing to the favorable ambiguity function properties and the increased deployment, mobile communications systems are useful for passive bistatic radar applications. Further, simultaneously using multiple illuminators in a multistatic configuration will improve the radar performance, providing spatial diversity and increased resolution. We compute modified Cramér-Rao lower bounds (MCRLB) for the target parameter (delay, Doppler) estimation error using universal mobile telecommunications system (UMTS) signals as illuminators of opportunity for passive multistatic radar systems. We consider both coherent and non-coherent processing modes. These expressions for MCRLB are an important performance metric in that they enable the selection of the optimal illuminators for estimation.**

***Index Terms*—Coherent processing, Cramér-Rao bound, distributed, multistatic, passive radar, UMTS signals.**

## I. Introduction

PASSIVE radar systems use several signals of opportunity as illuminators for target estimation unlike their active counterparts that require expensive transmission equipment. Some examples of these signals include television [1], [2], audio broadcast signals, FM radio [3], [4] and mobile communications systems [5]. By employing just the receivers, these systems are inherently robust and not detectable [6]–[8]. With their wide spread availability, mobile communications signals are important illuminators of opportunity. Further, employing passive radar systems in a multistatic configuration provides spatial diversity and improves the resolution [9] similar to the concept of active MIMO radar systems [10]–[13]. These passive multistatic radar systems view the targets from different aspect angles illuminated by different transmitters.

UMTS is a third generation wireless communications standard. These signals have been shown to provide good resolution as an illuminator for passive bistatic radar systems. [14] covers a detailed ambiguity function analysis using these illuminators in bistatic configuration to study the global resolution performance in terms of mainlobe width and sidelobes. Further, it also computes the bistatic MCRLB for these systems. CRLB is important for analyzing the local estimation accuracy as it provides a lower bound on the error variance of unbiased estimators. Further, under certain conditions, the maximum likelihood estimators (MLE) asymptotically achieve the CRLB [15]–[17]. While non-coherently combining the data from different constituent bistatic pairs provides spatial diversity gain, whenever phase synchronization is possible, these systems can be used for coherent processing to obtain very high resolution properties.

In this paper, we will compute the MCRLB [18] on the target estimation/localization using UMTS based passive multistatic radar under both coherent and non-coherent processing scenarios. Since the transmitted symbols are not deterministic, it is difficult to compute the classical CRLB. Therefore, we shall use the MCRLB as an alternative approach here by averaging the Fisher information matrix over the probability mass function of the transmitted symbol. In [19], [20], MCRLB has been studied and applied to radar problems. In [14], the authors computed the MCRLB for passive bistatic radar using UMTS signals. For the non-coherent processing mode, we will compute the modified Fisher information matrix (MFIM) by incorporating the UMTS passive bistatic radar results of [14] into the CRLB analysis for non-coherent MIMO radar described in [21]. For the coherent processing mode, in this paper we will derive closed-form expressions for the MFIM by computing the expected values of all the second order derivatives of the log-likelihood function.

Our MCRLB analysis will provide a quantitative measure of passive multistatic radar performance. The expressions will not just be a function of the transmitted waveforms but also a function of the multistatic radar-target geometry. The geometry has been shown to play a very important role in determining the bistatic ambiguity function [22], thereby also impacting the bistatic CRLB. While passive radar does not offer the freedom of designing the transmitted waveforms, it does allow flexibility in selecting the transmitters from among several choices. The geometry-dependent MCRLB analysis will open up a new dimension for passive multistatic radar systems by aiding the selection of optimal illuminators of opportunity to achieve a desired target estimation accuracy.

The rest of the paper is organized as follows. In Section II, we present the non-coherent and coherent measurement model for passive multistatic radar. In Section III, we will compute the expressions for the MFIM for the non-coherent scenario followed by the coherent scenario in Section IV. We will present some numerical examples to demonstrate our analytical results

Manuscript received March 11, 2013; revised August 10, 2013; accepted September 29, 2013. Date of publication October 04, 2013; date of current version December 05, 2013. The associate editor coordinating the review of this manuscript and approving it for publication was Prof. Ljubisa Stankovic. This work was supported by the Air Force Office of Scientific Research under Project 2311IN as LRIR 13RY10COR. The work of A. Nehorai was supported by AFOSR Grant FA9550-11-1-0210.

S. Gogineni is with the Wright State Research Institute, OH USA (e-mail: sandeep.gogineni@wright.edu).

M. Rangaswamy is with the Air Force Research Laboratory, Wright Patterson Air Force Base, OH USA (e-mail: Muralidhar.Rangaswamy@us.af.mil).

B. Rigling is with the Department of Electrical Engineering, Wright State University, Dayton, OH 45431 USA (e-mail: brian.rigling@wright.edu).

A. Nehorai is with the Preston M. Green Department of Electrical and Systems Engineering, Washington University, St. Louis, MO 63130 USA (e-mail: nehorai@ese.wustl.edu).

Color versions of one or more of the figures in this paper are available online at http://ieeexplore.ieee.org.

Digital Object Identifier 10.1109/TSP.2013.2284758

# Report Documentation Page

*Form Approved*
*OMB No. 0704-0188*



| | | |
|---|---|---|
| 1. REPORT DATE<br>**01 JAN 2014** | 2. REPORT TYPE | 3. DATES COVERED<br>**00-00-2014 to 00-00-2014** |
| 4. TITLE AND SUBTITLE<br>**Cramer-Rao Bounds for UMTS-Based Passive Multistatic Radar** | | 5a. CONTRACT NUMBER<br>5b. GRANT NUMBER<br>5c. PROGRAM ELEMENT NUMBER |
| 6. AUTHOR(S) | | 5d. PROJECT NUMBER<br>5e. TASK NUMBER<br>5f. WORK UNIT NUMBER |
| 7. PERFORMING ORGANIZATION NAME(S) AND ADDRESS(ES)<br>**Air Force Research Laboratory,Wright Patterson AFB,OH,45433** | | 8. PERFORMING ORGANIZATION REPORT NUMBER |
| 9. SPONSORING/MONITORING AGENCY NAME(S) AND ADDRESS(ES) | | 10. SPONSOR/MONITOR’S ACRONYM(S)<br>11. SPONSOR/MONITOR’S REPORT NUMBER(S) |

12. DISTRIBUTION/AVAILABILITY STATEMENT
**Approved for public release; distribution unlimited**

13. SUPPLEMENTARY NOTES

14. ABSTRACT
**Owing to the favorable ambiguity function properties and the increased deployment, mobile communications systems are useful for passive bistatic radar applications. Further, simultaneously using multiple illuminators in a multistatic configuration will improve the radar performance, providing spatial diversity and increased resolution. We compute modified Cram?r-Rao lower bounds (MCRLB) for the target parameter (delay, Doppler) estimation error using universal mobile telecommunications system (UMTS) signals as illuminators of opportunity for passive multistatic radar systems. We consider both coherent and non-coherent processing modes. These expressions for MCRLB are an important performance metric in that they enable the selection of the optimal illuminators for estimation.**

15. SUBJECT TERMS

| 16. SECURITY CLASSIFICATION OF: | | | 17. LIMITATION OF ABSTRACT | 18. NUMBER OF PAGES | 19a. NAME OF RESPONSIBLE PERSON |
|---|---|---|---|---|---|
| a. REPORT<br>**unclassified** | b. ABSTRACT<br>**unclassified** | c. THIS PAGE<br>**unclassified** | **Same as Report (SAR)** | **12** | |

in Section V. We shall demonstrate that the MCRLB is significantly lower for the coherent processing case than the non-coherent processing case. Further, we will demonstrate the dependence of the MCRLB values on the multistatic geometry. Finally, we provide concluding remarks with potential future work in Section VI.

## II. Signal Model

Consider a system comprising of $M_{\rm T}$ transmitters and $M_{\rm R}$ receivers. Let the $i^{th}$ transmitter be located at $\overrightarrow{\boldsymbol{t}_i} = [t_{xi}, t_{yi}]$. Similarly, the $j^{th}$ receiver is located at $\overrightarrow{\boldsymbol{r}_j} = [r_{xj}, r_{yj}]$. The target location and velocity are represented by

$$\overrightarrow{\boldsymbol{p}} = [p_x, p_y], \tag{1}$$
$$\overrightarrow{\boldsymbol{v}} = [v_x, v_y]. \tag{2}$$

Note that we chose the vectors from the 2-dimensional Cartesian space for simplicity. The results can easily be extended to the 3-dimensional space without loss of generality. Therefore, we define the target state vector

$$\mu = [p_x, p_y, v_x, v_y]. \tag{3}$$

Note that in the rest of the paper, we restrict our analysis to the single target scenario. In the presence of multiple targets, the number of unknown variables in the target parameter vector increases by a factor equal to the number of targets, thereby making the analysis much more complex. In future work, we will extend the analysis to the multiple target scenario by appending the parameters corresponding to multiple targets into the parameter vector. The baseband signal corresponding to the $i^{th}$ transmitter

$$u_i(t) = \frac{1}{\sqrt{N}} \sum_{n=0}^{N-1} c_{in} g_i(t - nT), \tag{4}$$

where $c_{in}$ are the transmitted quadrature phase shift keying (QPSK) symbols, $N$ is the number of symbols and $T$ is the inverse of the chip rate. The pulse $g_i(t)$ is defined as delayed root-raised-cosine (RRC) pulse $g_i(t) = h_i\left(t - \frac{D}{2}\right)$, where the delay $D$ and $h_i(t)$ are defined in [14].

Let $\tau_{ij}^{\mu}$ and $f_{{\rm D}_{ij}}^{\mu}$ denote the different bistatic delays and Doppler shifts associated with the target located at $\mu$:

$$\tau_{ij}^{\mu} = \frac{1}{c}\left(\|\overrightarrow{\boldsymbol{p}} - \overrightarrow{\boldsymbol{t}_i}\| + \|\overrightarrow{\boldsymbol{p}} - \overrightarrow{\boldsymbol{r}_j}\|\right), \tag{5}$$
$$f_{{\rm D}_{ij}}^{\mu} = \frac{f_{\rm ci}}{c}\left(\langle\overrightarrow{\boldsymbol{v}}, \overrightarrow{\boldsymbol{u}}_{\boldsymbol{r}_j}\rangle - \langle\overrightarrow{\boldsymbol{v}}, \overrightarrow{\boldsymbol{u}}_{\boldsymbol{t}_i}\rangle\right), \tag{6}$$

where $c$ represents the speed of wave propagation in the medium and $f_{\rm c}$ represents the carrier frequency. These transformation relations between the delay-Doppler space and the Cartesian coordinates are necessary while computing the MCRLB.

## III. Non-Coherent MCRLB

In this section, we will compute the MCRLB for the non-coherent processing scenario by deriving the MFIM expression. Under this scenario, the target is made up of several individual isotropic scatterers [11]. The target attenuations vary with the angle of view and the widely spaced antennas decorrelate these attenuations into uncorrelated zero-mean complex Gaussian random variables. If the target RCS values corresponding to certain bistatic pairs are weak, it is highly likely that they will be compensated for by other pairs with strong returns. We will recollect the expressions for the multistatic radar measurement vector using non-coherent processing. Note that the signals from different transmitters are assumed to be separable at the receivers in some domain (for example different frequency spectra). Therefore, we have $M_{\rm T}M_{\rm R}$ components of the received signals.

$$y_{ij}^{\mu}(t) = \beta_{ij} u_i\left(t - \tau_{ij}^{\mu}\right) e^{j2\pi\left(f_{{\rm D}_{ij}}^{\mu}\left(t - \tau_{ij}^{\mu}\right)\right)} + n_{ij}(t). \tag{7}$$

Note that $y_{ij}^{\mu}(t)$ are statistically independent for different transmitter-receiver pairs because of the wide separation between the antennas that leads to independent looks of the target. Let $n_{ij}(t)$ denote the additive zero-mean white Gaussian noise with variance $\sigma_n^2$. Further, the target attenuations $\beta_{ij}$ are zero-mean Gaussian distributed with variance $\sigma^2$.

Note that the transmitted symbol is not deterministic. Therefore, we will average the Fisher information matrix over the probability mass function of the transmitted symbol $\boldsymbol{c}$. First, for a given $\boldsymbol{c}$, the log-likelihood ratio across all transceiver pairs [21]–[24]

$$\log l\left(\boldsymbol{y}^{\mu}(t)|\boldsymbol{c}\right) = \sum_{i=1}^{M_{\rm T}} \sum_{j=1}^{M_{\rm R}} \log l\left(y_{ij}^{\mu}(t)|\boldsymbol{c}\right), \tag{8}$$

where

$$l\left(y_{ij}^{\mu}(t)|\boldsymbol{c}\right) = \frac{\sigma_n^2}{\sigma^2 + \sigma_n^2} e^{\sigma^2/\sigma_n^2\left(\sigma^2+\sigma_n^2\right)} \times e^{\left|\int_{-\infty}^{\infty} y_{ij}^{\mu}(t) u_i^*\left(t-\tau_{ij}^{\mu}\right) e^{-j2\pi\left(f_{{\rm D}_{ij}}^{\mu}\left(t-\tau_{ij}^{\mu}\right)\right)} {\rm d}t\right|^2}.$$

Therefore,

$$\log l\left(y_{ij}^{\mu}(t)|\boldsymbol{c}\right) = \frac{\sigma^2}{\sigma_n^2\left(\sigma^2 + \sigma_n^2\right)} \left|\int_{-\infty}^{\infty} y_{ij}^{\mu}(t) \times u_i^*\left(t - \tau_{ij}^{\mu}\right) e^{-j2\pi\left(f_{{\rm D}_{ij}}^{\mu}\left(t-\tau_{ij}^{\mu}\right)\right)} {\rm d}t\right|^2 + {\rm C},$$

where C is independent of the target state vector $\mu$. Note that the carrier dependent phase term is not present because it is absorbed into the circularly symmetric Gaussian distributed attenuation terms and does not impact the non-coherent processing.

Given this statistical model, the expression for the Fisher information matrix for non-coherent MIMO radar with widely separated antennas was derived in [21]. Using the relationships between the delay terms and the Cartesian coordinates,

$$\frac{\partial \tau_{ij}^{\mu}}{\partial p_x} = \frac{1}{c}\left(\frac{p_x - t_{xi}}{\|\overrightarrow{\boldsymbol{p}} - \overrightarrow{\boldsymbol{t}_i}\|} + \frac{p_x - r_{xj}}{\|\overrightarrow{\boldsymbol{p}} - \overrightarrow{\boldsymbol{r}_j}\|}\right),$$
$$\frac{\partial \tau_{ij}^{\mu}}{\partial p_y} = \frac{1}{c}\left(\frac{p_y - t_{yi}}{\|\overrightarrow{\boldsymbol{p}} - \overrightarrow{\boldsymbol{t}_i}\|} + \frac{p_y - r_{yj}}{\|\overrightarrow{\boldsymbol{p}} - \overrightarrow{\boldsymbol{r}_j}\|}\right).$$

Similarly, the relations between the Doppler shift terms and the Cartesian coordinates for target position and velocity give [21]

$$\frac{\partial f^{\mu}_{\mathrm{D}_{ij}}}{\partial p_x} = \frac{-v_x}{\lambda}\left(\frac{1}{\|\overrightarrow{\boldsymbol{p}} - \overrightarrow{\boldsymbol{t}_i}\|} + \frac{1}{\|\overrightarrow{\boldsymbol{p}} - \overrightarrow{\boldsymbol{r}_j}\|}\right) + \frac{t_{xi} - p_x}{\lambda\|\overrightarrow{\boldsymbol{p}} - \overrightarrow{\boldsymbol{t}_i}\|^3} \left(v_x\left(t_{xi} - p_x\right) + v_y\left(t_{yi} - p_y\right)\right) + \frac{r_{xj} - p_x}{\lambda\|\overrightarrow{\boldsymbol{p}} - \overrightarrow{\boldsymbol{r}_j}\|^3} \left(v_x\left(r_{xj} - p_x\right) + v_y\left(r_{yj} - p_y\right)\right),$$

and

$$\frac{\partial f^{\mu}_{\mathrm{D}_{ij}}}{\partial p_y} = \frac{-v_y}{\lambda}\left(\frac{1}{\|\overrightarrow{\boldsymbol{p}} - \overrightarrow{\boldsymbol{t}_i}\|} + \frac{1}{\|\overrightarrow{\boldsymbol{p}} - \overrightarrow{\boldsymbol{r}_j}\|}\right) + \frac{t_{yi} - p_y}{\lambda\|\overrightarrow{\boldsymbol{p}} - \overrightarrow{\boldsymbol{t}_i}\|^3} \left(v_x\left(t_{xi} - p_x\right) + v_y\left(t_{yi} - p_y\right)\right) + \frac{r_{yj} - p_y}{\lambda\|\overrightarrow{\boldsymbol{p}} - \overrightarrow{\boldsymbol{r}_j}\|^3} \left(v_x\left(r_{xj} - p_x\right) + v_y\left(r_{yj} - p_y\right)\right),$$

where $\lambda$ denotes the carrier wavelength, and

$$\frac{\partial f^{\mu}_{\mathrm{D}_{ij}}}{\partial v_x} = \frac{t_{xi} - p_x}{\lambda\|\overrightarrow{\boldsymbol{p}} - \overrightarrow{\boldsymbol{t}_i}\|} + \frac{r_{xj} - p_x}{\lambda\|\overrightarrow{\boldsymbol{p}} - \overrightarrow{\boldsymbol{r}_j}\|},$$

$$\frac{\partial f^{\mu}_{\mathrm{D}_{ij}}}{\partial v_y} = \frac{t_{yi} - p_y}{\lambda\|\overrightarrow{\boldsymbol{p}} - \overrightarrow{\boldsymbol{t}_i}\|} + \frac{r_{yj} - p_y}{\lambda\|\overrightarrow{\boldsymbol{p}} - \overrightarrow{\boldsymbol{r}_j}\|}.$$

The analysis for non-coherent MIMO radar in [21] expresses the MIMO FIM as a combination of the constituent bistatic FIMs. Therefore, we can express the MFIM for our problem as

$$\boldsymbol{J}(\mu) = \frac{8\pi^2\sigma^4}{\left(\sigma^2 + \sigma_n^2\right)\sigma_n^2}\sum_{i=1}^{M_{\mathrm{T}}}\sum_{j=1}^{M_{\mathrm{R}}}\tilde{\boldsymbol{J}}_{ij}(\mu), \tag{9}$$

where the final expressions for the elements of the symmetric Fisher information matrix $\tilde{\boldsymbol{J}}_{ij}(\mu)$ corresponding to the $ij^{th}$ transceiver pair are given in Appendix using the bistatic results from [14] and the equations for the transformation of variables described above. Note that since the transmitted waveforms $u_i(t)$ are not deterministic, expected values of the entries of FIM were used to arrive at the expressions in the Appendix. This is in contrast to the classical CRLB that needs us to average across the transmitted waveform space in the joint probability density function of the measurement vector $\boldsymbol{y}^{\mu}(t)$ instead of the conditional density function. Computing the classical CRLB is not feasible for our problem [14]. However, MCRLB has been studied and applied to radar problems earlier [19], [20] as it provides a good benchmark when computing the classical CRLB is not feasible. Finally we will invert this modified FIM to obtain the modified CRLB as the diagonal entries of $\boldsymbol{J}^{-1}(\mu)$. We clearly observe from the expressions of the entries of the modified FIM (in the Appendix) that the MCRLB depends on the multistatic geometry along with the transmitted waveform parameters $\alpha_i$, thereby making the choice of transmitters important.

## IV. COHERENT MCRLB

Having computed the MCRLB for the non-coherent processing scenario, we move on to the coherent processing mode. In this mode, the target attenuations are made up of a single point scatterer that has an isotropic complex reflectivity denoted by $\beta = \beta_{\mathrm{Re}} + j\beta_{\mathrm{Im}}$[10]. Further, this attenuation coefficient is a deterministic unknown quantity unlike the random Gaussian modeling in the non-coherent case. Therefore, we modify the target state vector to include the attenuation coefficients $\mu = [p_x, p_y, v_x, v_y, \beta_{\mathrm{Re}}, \beta_{\mathrm{Im}}]$. An alternative representation of the target state vector in the delay-Doppler domain is $\nu = \left[\tau^{\mu}_{11}, \ldots, \tau^{\mu}_{M_{\mathrm{T}}M_{\mathrm{R}}}, f^{\mu}_{\mathrm{D}_{11}}, \ldots, f^{\mu}_{\mathrm{D}_{M_{\mathrm{T}}M_{\mathrm{R}}}}, \beta_{\mathrm{Re}}, \beta_{\mathrm{Im}}\right]$. We will use the representation given by $\nu$ as an interim step before computing the MCRLB.

Since we have assumed that the different transmitted signals are separable at the receivers (different carrier frequencies/resources), the received signal corresponding to the $i^{th}$ transmitter and the $j^{th}$ receiver for the coherent processing scenario can be given as

$$y^{\mu}_{ij}(t) = \beta u_i\left(t - \tau^{\mu}_{ij}\right) e^{j2\pi\left(f^{\mu}_{\mathrm{D}_{ij}}\left(t-\tau^{\mu}_{ij}\right) - f_{\mathrm{c}i}\tau^{\mu}_{ij}\right)} + n_{ij}(t).$$

Note the presence of the phase term $e^{-j2\pi f_{\mathrm{c}i}\tau^{\mu}_{ij}}$ in the above expression. The CRLB for coherent MIMO radar with stationary targets was computed in [25]–[27]. Recently, moving targets were considered in [28].

The log-likelihood function across all receivers for a given transmitted waveform

$$\log l\left(\boldsymbol{y}^{\mu}(t)|\boldsymbol{c}\right) = \sum_{i=1}^{M_{\mathrm{T}}}\sum_{j=1}^{M_{\mathrm{R}}} \log l\left(y^{\mu}_{ij}(t)|\boldsymbol{c}\right), \tag{10}$$

where

$$l\left(y^{\mu}_{ij}(t)|\boldsymbol{c}\right) \propto e^{-\frac{1}{\sigma_n^2}\int_{-\infty}^{\infty}\left|y^{\mu}_{ij}(t) - \beta u_i\left(t-\tau^{\mu}_{ij}\right)e^{j2\pi\left(f^{\mu}_{\mathrm{D}_{ij}}\left(t-\tau^{\mu}_{ij}\right) - f_{\mathrm{c}i}\tau^{\mu}_{ij}\right)}\right|^2 \mathrm{d}t}.$$

Therefore,

$$\log l\left(\boldsymbol{y}^{\mu}(t)|\boldsymbol{c}\right) = -\frac{1}{\sigma_n^2}\sum_{i=1}^{M_{\mathrm{T}}}\sum_{j=1}^{M_{\mathrm{R}}}\int_{-\infty}^{\infty}\left|y^{\mu}_{ij}(t) - \beta u_i\left(t-\tau^{\mu}_{ij}\right) e^{j2\pi\left(f^{\mu}_{\mathrm{D}_{ij}}\left(t-\tau^{\mu}_{ij}\right) - f_{\mathrm{c}i}\tau^{\mu}_{ij}\right)}\right|^2 \mathrm{d}t + \mathrm{C}.$$

This simplifies to

$$\begin{aligned}\log l\left(\boldsymbol{y}^{\mu}(t)|\boldsymbol{c}\right) = & -\frac{1}{\sigma_n^2}\sum_{i=1}^{M_{\mathrm{T}}}\sum_{j=1}^{M_{\mathrm{R}}}\int_{-\infty}^{\infty}\Bigg(\left(y^{\mu}_{ij}(t)\right)^* y^{\mu}_{ij}(t) \\ & - \beta\left(y^{\mu}_{ij}(t)\right)^* u_i\left(t-\tau^{\mu}_{ij}\right) e^{j2\pi\left(f^{\mu}_{\mathrm{D}_{ij}}\left(t-\tau^{\mu}_{ij}\right) - f_{\mathrm{c}i}\tau^{\mu}_{ij}\right)} \\ & + |\beta|^2 u_i^*\left(t-\tau^{\mu}_{ij}\right) u_i\left(t-\tau^{\mu}_{ij}\right) e^{-j2\pi\left(f^{\mu}_{\mathrm{D}_{ij}}\left(t-\tau^{\mu}_{ij}\right) - f_{\mathrm{c}i}\tau^{\mu}_{ij}\right)} e^{j2\pi\left(f^{\mu}_{\mathrm{D}_{ij}}\left(t-\tau^{\mu}_{ij}\right) - f_{\mathrm{c}i}\tau^{\mu}_{ij}\right)} \\ & - \beta^* y^{\mu}_{ij}(t) u_i^*\left(t-\tau^{\mu}_{ij}\right) e^{-j2\pi\left(f^{\mu}_{\mathrm{D}_{ij}}\left(t-\tau^{\mu}_{ij}\right) - f_{\mathrm{c}i}\tau^{\mu}_{ij}\right)}\Bigg)\mathrm{d}t + \mathrm{C},\end{aligned}$$

where C is a constant independent of the target state vector $\mu$.

The third term reduces to

$$|\beta|^2 \sum_{i=1}^{M_{\mathrm{T}}} \int_{-\infty}^{\infty} u_i^* \left(t - \tau_{ij}^{\mu}\right) u_i \left(t - \tau_{ij}^{\mu}\right) \mathrm{d}t = |\beta|^2. \tag{11}$$

Note that we are considering unit energy complex envelopes for the QPSK transmitted waveforms shaped by RRC filters as given in [14]. Further, the first term is purely a function of the measurements and does not contain the delay, Doppler, and attenuation parameters. Hence,

$$\log l \left(\boldsymbol{y}^{\mu}(t) | \boldsymbol{c}\right) = \frac{2}{\sigma_n^2} \sum_{i=1}^{M_{\mathrm{T}}} \sum_{j=1}^{M_{\mathrm{R}}} \int_{-\infty}^{\infty} \left( \mathrm{Re}\left\{ \beta^* y_{ij}^{\mu}(t) \right.\right.$$
$$\left.\left. u_i^* \left(t - \tau_{ij}^{\mu}\right) e^{-j2\pi \left( f_{\mathrm{D}_{ij}}^{\mu} \left(t - \tau_{ij}^{\mu}\right) - f_{\mathrm{c}i} \tau_{ij}^{\mu} \right)} \right\} \right) \mathrm{d}t$$
$$- \frac{M_{\mathrm{T}} M_{\mathrm{R}} |\beta|^2}{\sigma_n^2} + \mathrm{C}',$$

where $\mathrm{C}'$ is another constant.

It is easier to compute the MFIM in the $\nu$ domain and then apply a change of variables transformation to the $\mu$ space. Therefore, we have

$$\boldsymbol{J}(\mu) = \left(\frac{\partial \nu}{\partial \mu}\right) \boldsymbol{J}(\nu) \left(\frac{\partial \nu}{\partial \mu}\right)^T. \tag{12}$$

First, we need to compute the term $\frac{\partial \nu}{\partial \mu}$ that corresponds to the change of variables. In this term, we have already stated the expressions for the derivatives of the delay and Doppler terms with respect to the Cartesian positions and velocities in the non-coherent processing section. The terms that are new for this coherent scenario are the derivatives with respect to the attenuations $\beta_{\mathrm{Re}}$ and $\beta_{\mathrm{Im}}$. Since the delays and Dopplers do not depend on these terms, these derivatives are

$$\frac{\partial \tau_{ij}^{\mu}}{\partial \beta_{\mathrm{Re}}} = 0, \frac{\partial \tau_{ij}^{\mu}}{\partial \beta_{\mathrm{Im}}} = 0, \frac{\partial f_{\mathrm{D}_{ij}}^{\mu}}{\partial \beta_{\mathrm{Re}}} = 0, \frac{\partial f_{\mathrm{D}_{ij}}^{\mu}}{\partial \beta_{\mathrm{Im}}} = 0.$$

Additionally, we also have

$$\frac{\partial \beta_{\mathrm{Re}}}{\partial p_x} = 0, \frac{\partial \beta_{\mathrm{Im}}}{\partial p_x} = 0, \frac{\partial \beta_{\mathrm{Re}}}{\partial p_y} = 0, \frac{\partial \beta_{\mathrm{Im}}}{\partial p_y} = 0,$$
$$\frac{\partial \beta_{\mathrm{Re}}}{\partial v_x} = 0, \frac{\partial \beta_{\mathrm{Im}}}{\partial v_x} = 0, \frac{\partial \beta_{\mathrm{Re}}}{\partial v_y} = 0, \frac{\partial \beta_{\mathrm{Im}}}{\partial v_y} = 0,$$
$$\frac{\partial \beta_{\mathrm{Re}}}{\partial \beta_{\mathrm{Re}}} = 1, \frac{\partial \beta_{\mathrm{Re}}}{\partial \beta_{\mathrm{Im}}} = 0, \frac{\partial \beta_{\mathrm{Im}}}{\partial \beta_{\mathrm{Re}}} = 0, \frac{\partial \beta_{\mathrm{Im}}}{\partial \beta_{\mathrm{Im}}} = 1.$$

Now, the only matrix we need to compute for obtaining the MCRLB is $\boldsymbol{J}(\nu)$. We computed closed-form expressions for each entry of this matrix by evaluating all the second-order derivatives(see Appendix for the derivations). Using these expressions, we will compute the coherent MCRLB as the diagonal elements of $\mathrm{MCRLB}_{\mathrm{C}}(\mu) = \boldsymbol{J}^{-1}(\mu)$.

## V. Numerical Examples

In this section, we will use numerical examples to compute the MCRLB for a UMTS-based passive multistatic radar system. We consider 5 transmitters and 5 receivers (See Fig. 1) located at

$$\begin{aligned}
\overrightarrow{\boldsymbol{t}_1} &= [1.5, 2]\,\mathrm{km} \quad ; \quad \overrightarrow{\boldsymbol{r}_1} = [3, 0]\,\mathrm{km};\\
\overrightarrow{\boldsymbol{t}_2} &= [1.5, 2.25]\,\mathrm{km} \quad ; \quad \overrightarrow{\boldsymbol{r}_2} = [5, 0]\,\mathrm{km};\\
\overrightarrow{\boldsymbol{t}_3} &= [1.5, 2.5]\,\mathrm{km} \quad ; \quad \overrightarrow{\boldsymbol{r}_3} = [0, 3.5]\,\mathrm{km};\\
\overrightarrow{\boldsymbol{t}_4} &= [2, 1.5]\,\mathrm{km} \quad ; \quad \overrightarrow{\boldsymbol{r}_4} = [1, 1]\,\mathrm{km};\\
\overrightarrow{\boldsymbol{t}_5} &= [2, 1.75]\,\mathrm{km} \quad ; \quad \overrightarrow{\boldsymbol{r}_5} = [4, 4]\,\mathrm{km}.
\end{aligned}$$

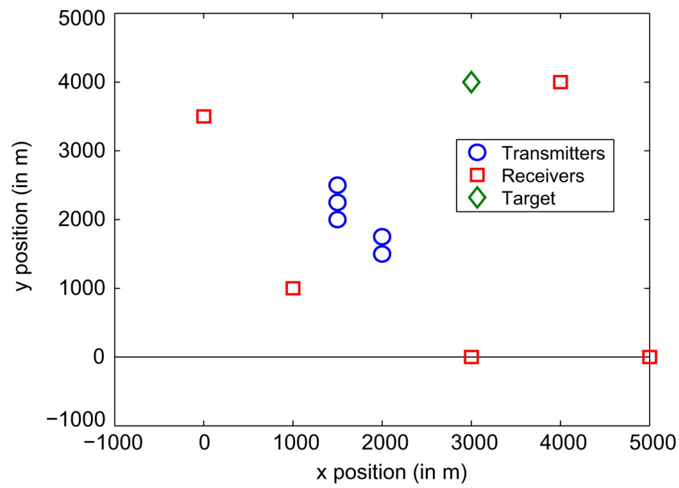


Fig. 1. Simulated multistatic scenario with Transmitter and receiver locations.

We will compute the square root of MCRLB (RMCRLB) around the position $[3, 4]$ km and velocity $[30, 50]$ m/s. We chose the same system parameters as in [14] for the simulations; observation time $NT = 0.1$s, $T = 0.26$ $\mu$s, $\alpha = 0.22$, and the center frequency $f_{\mathrm{c}} = 2100$ MHz. Define the signal-to-noise ratio (SNR) as

$$\mathrm{SNR} = 10 \log \left(\frac{\sigma^2}{\sigma_n^2}\right). \tag{13}$$

In Fig. 2, we plotted the non-coherent RMCRLB in the x-position and y-position dimensions as a function of the SNR. Similarly, Fig. 3 shows the velocity RMCRLB for varying SNR. We observe that the RMCRLB is lower in the y-dimension for both the position and velocity. At an SNR of 0 dB, the RMCRLB for the x and y positions are $9.6206$ m and $4.8496$ m, respectively. The RMCRLB for the x and y velocities at the same SNR are $0.1727$ m/s and $0.1121$ m/s, respectively. Now, to show the importance of the geometry, we change the position for which we are computing the RMCRLB to $[3, 1.5]$ km. While this does not affect the terms $E\{\epsilon_i\}$, $E\{\gamma_{ij}\}$, and $E\{\eta_{ij}\}$, it impacts the derivatives of the delay-Doppler terms with respect to the Cartesian coordinates. We clearly observe from Fig. 4 that the RMCRLB at 0 dB SNR for $p_x$ is $5.5077$ m and that for $p_y$ is $5.1567$ m. These numbers are different from the earlier case and the same holds true even for the velocity RMCRLB.

For the coherent processing scenario, we choose $\beta = \frac{1+\sqrt{-1}}{\sqrt{2}}$. Therefore, the signal-to-noise ratio

$$\mathrm{SNR} = 10 \log \left(\frac{1}{\sigma_n^2}\right). \tag{14}$$

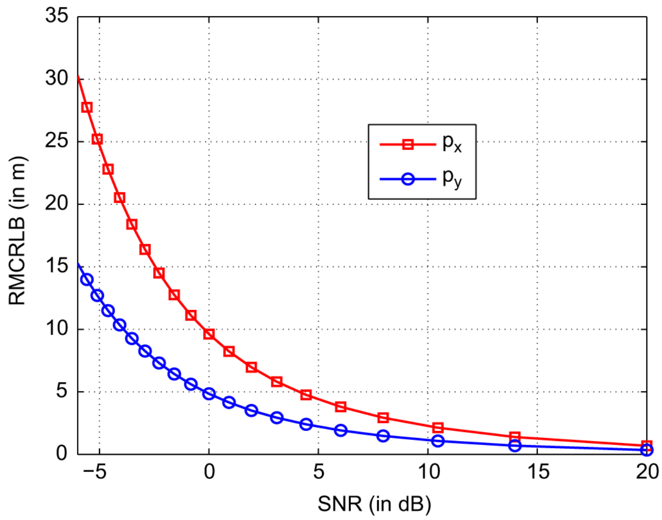


Fig. 2. Non-coherent RMCRLB in the x-position and y-position dimensions as a function of SNR.

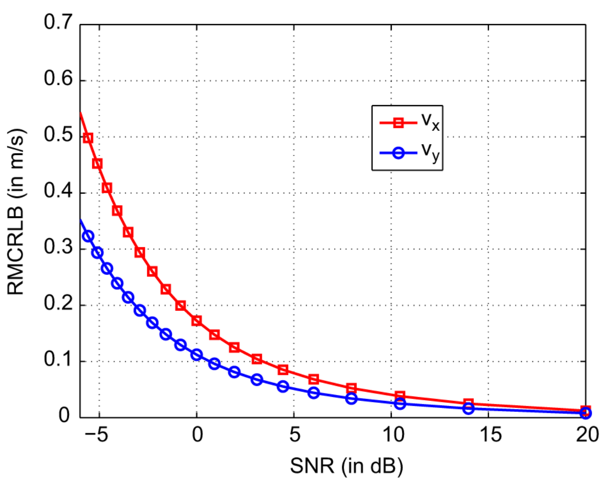


Fig. 3. Non-coherent RMCRLB in the x-velocity and y-velocity dimensions as a function of SNR.

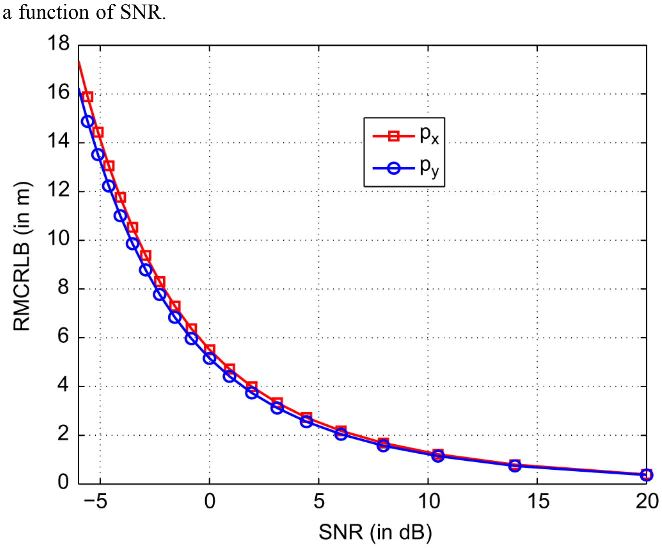


Fig. 4. Non-coherent RMCRLB in the x-position and y-position dimensions as a function of SNR when $[p_x, p_y] = [3, 1.5]$ km .

We plotted the RMCRLB curves using the same parameters as the non-coherent case around the position $[3, 4]$ km and velocity

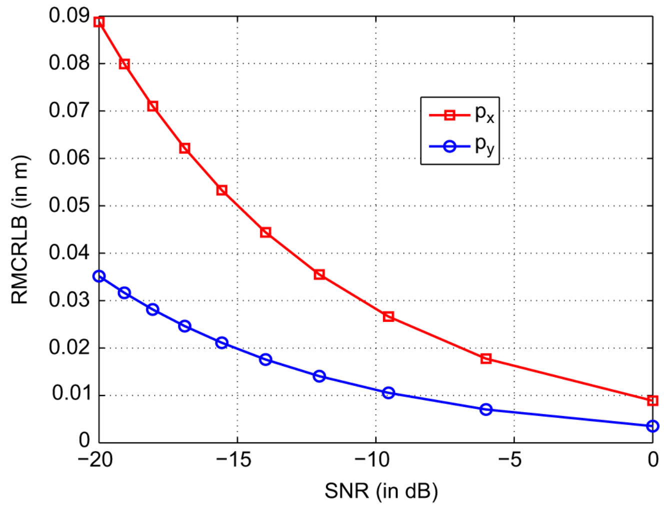


Fig. 5. Coherent RMCRLB in the x-position and y-position dimensions as a function of SNR.

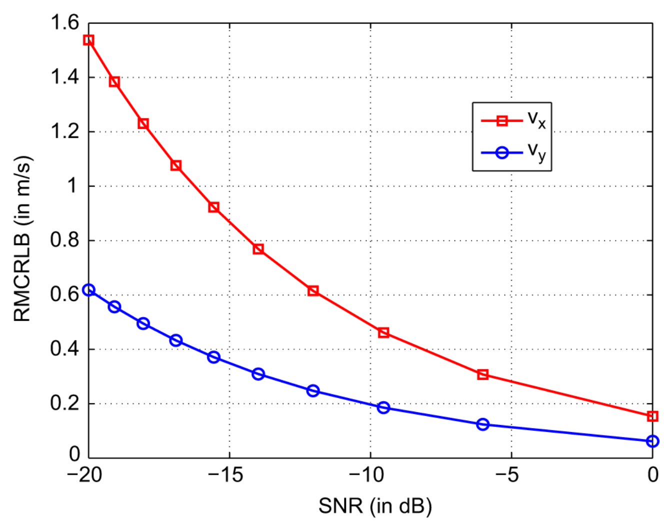


Fig. 6. Coherent RMCRLB in the x-velocity and y-velocity dimensions as a function of SNR.

$[30, 50]$ m/s. In Fig. 5, we plot the RMCRLB for both the position parameters. We clearly notice that the RMCRLB is much lower when compared with the non-coherent case.

Next, we plotted the RMCRLB for the velocity parameters in Fig. 6. Even here, the CRLB is significantly lower when compared with the non-coherent scenario. At an SNR of $-6$ dB, the coherent velocity RMCRLB in x and y dimensions are $0.3076$ m/s and $0.1237$ m/s, respectively as opposed to $0.5460$ m/s and $0.3545$ m/s for the non-coherent case. For the coherent case, there are additional unknown parameters other than the positions and velocities in the form of $\beta$. In Fig. 7, we plot the RMCRLB for $\beta_{\text{Re}}$ and $\beta_{\text{Im}}$ as a function of the SNR. Just as we did for the non-coherent case, we will change the position to different value and demonstrate the dependence of the RMCRLB values on the geometry. Let the true position parameters be $[6, 2.5]$ km. Fig. 8 demonstrates the change in values of RMCRLB when compared to the previous geometry in Fig. 5. When the true position is $[6, 2.5]$ km, we observe that the x-position dimension has a lower RMCRLB than the y-position dimension. This is contrary to the scenario when the true target position was $[3, 4]$ km. In [14], the authors show that the bistatic RMCRLB shoots up rapidly as the target position

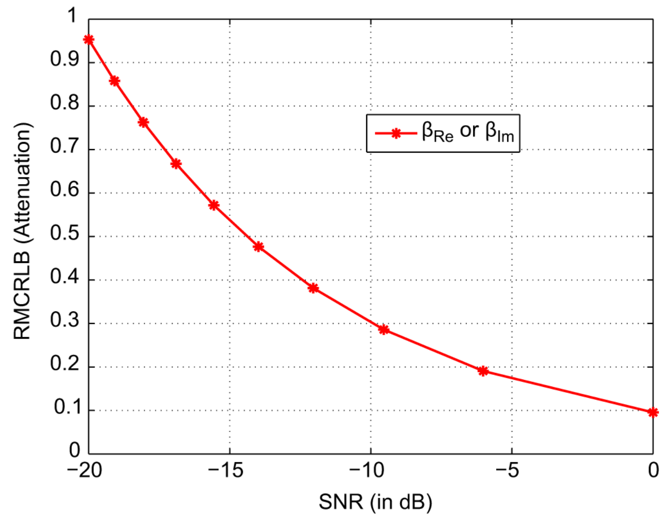


Fig. 7. Coherent RMCRLB in the attenuation dimensions as a function of SNR.

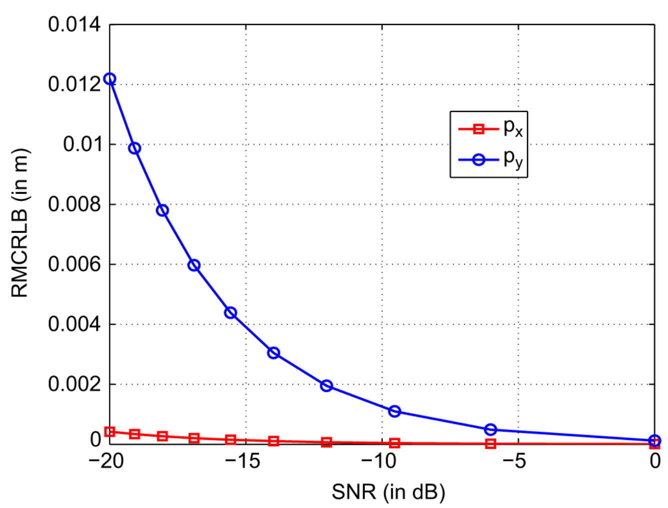


Fig. 8. Coherent RMCRLB in the x-position and y-position dimensions as a function of SNR when $[p_x, p_y] = [6, 2.5]$ km .

approaches the bistatic baseline. In the multistatic case, several constituent bistatic pairs affect the overall RMCRLB and hence it is more complex to study the dependence of these expressions on the geometry.

Note that even though the coherent processing mode offers lower RMCRLB than the non-coherent mode, these two scenarios represent two completely different target models. Therefore, coherent processing is not applicable when the target consists of multiple individual isotropic scatterers that cause uncorrelated phase shifts across different transceiver pairs. Further, it is very important to have perfect phase synchronization between all the transmitters and receivers for coherent processing and this is not always possible as a result of several physical limitations like inaccurate knowledge of the antenna locations and local oscillator characteristics [29]–[31].

## VI. Concluding Remarks

We have computed MCRLB for passive multistatic radar systems using the UMTS waveforms as the illuminators of opportunity by deriving closed-form expressions of the MFIM. We have considered both the non-coherent and coherent processing scenarios. We observe that the MCRLB is significantly lower for the coherent processing case than the non-coherent processing. Further, we demonstrated the dependence of the MCRLB values on the multistatic geometry. The MCRLB results validate the feasibility of using the UMTS signals as an important illuminator for passive radar.

In future work, we will extend this research by considering other illuminators of opportunity in addition to UMTS waveforms. Additionally, we will extend the analysis to the multiple target scenario by appending the parameters corresponding to multiple targets into the parameter vector and evaluating all the corresponding additional terms in the MFIM. Further, this would facilitate a way to solve the important problem of optimal illuminator selection for passive multistatic radar systems.

## Appendix

The entries of the constituent bistatic MFIM for the non-coherent processing scenario can be expressed as

$$\begin{aligned}
\tilde{J}_{ij}^{11}(\mu) &= \frac{1}{12T^2}\left(\frac{\partial \tau_{ij}^{\mu}}{\partial p_x}\right)^2\left(1+3\alpha_i^2-24\frac{\alpha_i^2}{\pi^2}\right) \\
&\quad + \frac{T^2}{4}\left(\frac{\partial f_{\mathrm{D}_{ij}}^{\mu}}{\partial p_x}\right)^2\left(\frac{1}{4\alpha_i}+\frac{N^2-1}{3}\right), \\
\tilde{J}_{ij}^{12}(\mu) &= \left(\frac{1}{12T^2}\frac{\partial \tau_{ij}^{\mu}}{\partial p_x}\left(1+3\alpha_i^2-24\frac{\alpha_i^2}{\pi^2}\right)\right)\frac{\partial \tau_{ij}^{\mu}}{\partial p_y} \\
&\quad + \left(\frac{T^2}{4}\frac{\partial f_{\mathrm{D}_{ij}}^{\mu}}{\partial p_x}\left(\frac{1}{4\alpha_i}+\frac{N^2-1}{3}\right)\right)\frac{\partial f_{\mathrm{D}_{ij}}^{\mu}}{\partial p_y}, \\
\tilde{J}_{ij}^{13}(\mu) &= \left(\frac{T^2}{4}\frac{\partial f_{\mathrm{D}_{ij}}^{\mu}}{\partial p_x}\left(\frac{1}{4\alpha_i}+\frac{N^2-1}{3}\right)\right)\frac{\partial f_{\mathrm{D}_{ij}}^{\mu}}{\partial v_x}, \\
\tilde{J}_{ij}^{14}(\mu) &= \left(\frac{T^2}{4}\frac{\partial f_{\mathrm{D}_{ij}}^{\mu}}{\partial p_x}\left(\frac{1}{4\alpha_i}+\frac{N^2-1}{3}\right)\right)\frac{\partial f_{\mathrm{D}_{ij}}^{\mu}}{\partial v_y}, \\
\tilde{J}_{ij}^{22}(\mu) &= \frac{1}{12T^2}\left(\frac{\partial \tau_{ij}^{\mu}}{\partial p_y}\right)^2\left(1+3\alpha_i^2-24\frac{\alpha_i^2}{\pi^2}\right) \\
&\quad + \frac{T^2}{4}\left(\frac{\partial f_{\mathrm{D}_{ij}}^{\mu}}{\partial p_y}\right)^2\left(\frac{1}{4\alpha_i}+\frac{N^2-1}{3}\right), \\
\tilde{J}_{ij}^{23}(\mu) &= \left(\frac{1}{12T^2}\frac{\partial f_{\mathrm{D}_{ij}}^{\mu}}{\partial p_y}\left(1+3\alpha_i^2-24\frac{\alpha_i^2}{\pi^2}\right)\right)\frac{\partial f_{\mathrm{D}_{ij}}^{\mu}}{\partial v_x}, \\
\tilde{J}_{ij}^{24}(\mu) &= \left(\frac{1}{12T^2}\frac{\partial f_{\mathrm{D}_{ij}}^{\mu}}{\partial p_y}\left(1+3\alpha_i^2-24\frac{\alpha_i^2}{\pi^2}\right)\right)\frac{\partial f_{\mathrm{D}_{ij}}^{\mu}}{\partial v_y}, \\
\tilde{J}_{ij}^{33}(\mu) &= \frac{T^2}{4}\left(\frac{\partial f_{\mathrm{D}_{ij}}^{\mu}}{\partial v_x}\right)^2\left(\frac{1}{4\alpha_i}+\frac{N^2-1}{3}\right), \\
\tilde{J}_{ij}^{34}(\mu) &= \frac{T^2}{4}\frac{\partial f_{\mathrm{D}_{ij}}^{\mu}}{\partial v_x}\frac{\partial f_{\mathrm{D}_{ij}}^{\mu}}{\partial v_y}\left(\frac{1}{4\alpha_i}+\frac{N^2-1}{3}\right), \\
\tilde{J}_{ij}^{44}(\mu) &= \frac{T^2}{4}\left(\frac{\partial f_{\mathrm{D}_{ij}}^{\mu}}{\partial v_y}\right)^2\left(\frac{1}{4\alpha_i}+\frac{N^2-1}{3}\right).
\end{aligned}$$

For the coherent processing scenario, first, we will compute $\frac{\partial \log l(\boldsymbol{y}^{\mu}(t)|\boldsymbol{c})}{\partial \tau_{ij}^{\mu}}$. Recollect from Section IV that the log-likelihood

$$\log l\left(\boldsymbol{y}^{\mu}(t)|\boldsymbol{c}\right) = \frac{2}{\sigma_n^2}\sum_{i=1}^{M_{\mathrm{T}}}\sum_{j=1}^{M_{\mathrm{R}}}\int_{-\infty}^{\infty}\left(\mathrm{Re}\left\{\beta^* y_{ij}^{\mu}(t) u_i^*\left(t-\tau_{ij}^{\mu}\right)e^{-j2\pi\left(f_{\mathrm{D}_{ij}}^{\mu}\left(t-\tau_{ij}^{\mu}\right)-f_{\mathrm{c}i}\tau_{ij}^{\mu}\right)}\right\}\right)\mathrm{d}t - \frac{M_{\mathrm{T}}M_{\mathrm{R}}|\beta|^2}{\sigma_n^2} + \mathrm{C}'.$$

We observe that the first and third terms in the above expression will be zero as they do not depend on the delay terms. Hence,

$$\frac{\partial \log l\left(\boldsymbol{y}^{\mu}(t)|\boldsymbol{c}\right)}{\partial \tau_{ij}^{\mu}} = \frac{2}{\sigma_n^2}\int_{-\infty}^{\infty}\left(\mathrm{Re}\left\{\beta^* y_{ij}^{\mu}(t)\frac{\partial u_i^*\left(t-\tau_{ij}^{\mu}\right)}{\partial \tau_{ij}^{\mu}}e^{-j2\pi\left(f_{\mathrm{D}_{ij}}^{\mu}\left(t-\tau_{ij}^{\mu}\right)-f_{\mathrm{c}i}\tau_{ij}^{\mu}\right)}\right\}\right)\mathrm{d}t + \frac{4\pi\left(f_{\mathrm{c}i}+f_{\mathrm{D}_{ij}}^{\mu}\right)}{\sigma_n^2}\int_{-\infty}^{\infty}\left(\mathrm{Re}\left\{j\beta^* y_{ij}^{\mu}(t)u_i^*\left(t-\tau_{ij}^{\mu}\right) \times e^{-j2\pi\left(f_{\mathrm{D}_{ij}}^{\mu}\left(t-\tau_{ij}^{\mu}\right)-f_{\mathrm{c}i}\tau_{ij}^{\mu}\right)}\right\}\right)\mathrm{d}t.$$

Next, we compute the derivative with respect to the Doppler shift term. Since the Doppler term only shows up in the carrier and not in the waveform term, we have

$$\frac{\partial \log l\left(\boldsymbol{y}^{\mu}(t)|\boldsymbol{c}\right)}{\partial f_{\mathrm{D}_{ij}}^{\mu}} = -\frac{4\pi}{\sigma_n^2}\int_{-\infty}^{\infty}\left(\mathrm{Re}\left\{j\beta^* y_{ij}^{\mu}(t)\left(t-\tau_{ij}^{\mu}\right) \times u_i^*\left(t-\tau_{ij}^{\mu}\right)e^{-j2\pi\left(f_{\mathrm{D}_{ij}}^{\mu}\left(t-\tau_{ij}^{\mu}\right)-f_{\mathrm{c}i}\tau_{ij}^{\mu}\right)}\right\}\right)\mathrm{d}t.$$

Finally, the first derivative w.r.t the attenuation terms

$$\frac{\partial \log l\left(\boldsymbol{y}^{\mu}(t)|\boldsymbol{c}\right)}{\partial \beta_{\mathrm{Re}}} = -\frac{2M_{\mathrm{T}}M_{\mathrm{R}}\beta_{\mathrm{Re}}}{\sigma_n^2} + \frac{2}{\sigma_n^2}\sum_{i=1}^{M_{\mathrm{T}}}\sum_{j=1}^{M_{\mathrm{R}}}\int_{-\infty}^{\infty}\left(\mathrm{Re}\left\{y_{ij}^{\mu}(t)u_i^*\left(t-\tau_{ij}^{\mu}\right) \times e^{-j2\pi\left(f_{\mathrm{D}_{ij}}^{\mu}\left(t-\tau_{ij}^{\mu}\right)-f_{\mathrm{c}i}\tau_{ij}^{\mu}\right)}\right\}\right)\mathrm{d}t,$$

and

$$\frac{\partial \log l\left(\boldsymbol{y}^{\mu}(t)|\boldsymbol{c}\right)}{\partial \beta_{\mathrm{Im}}} = -\frac{2M_{\mathrm{T}}M_{\mathrm{R}}\beta_{\mathrm{Im}}}{\sigma_n^2} + \frac{2}{\sigma_n^2}\sum_{i=1}^{M_{\mathrm{T}}}\sum_{j=1}^{M_{\mathrm{R}}}\int_{-\infty}^{\infty}\left(\mathrm{Im}\left\{y_{ij}^{\mu}(t)u_i^*\left(t-\tau_{ij}^{\mu}\right) \times e^{-j2\pi\left(f_{\mathrm{D}_{ij}}^{\mu}\left(t-\tau_{ij}^{\mu}\right)-f_{\mathrm{c}i}\tau_{ij}^{\mu}\right)}\right\}\right)\mathrm{d}t.$$

We have finished computing first order derivatives. However, the FIM needs the evaluation of the second-order derivatives.

We clearly observe that

$$\frac{\partial^2 \log l\left(\boldsymbol{y}^{\mu}(t)|\boldsymbol{c}\right)}{\partial {\beta_{\mathrm{Re}}}^2} = -\frac{2M_{\mathrm{T}}M_{\mathrm{R}}}{\sigma_n^2},$$
$$\frac{\partial^2 \log l\left(\boldsymbol{y}^{\mu}(t)|\boldsymbol{c}\right)}{\partial {\beta_{\mathrm{Im}}}^2} = -\frac{2M_{\mathrm{T}}M_{\mathrm{R}}}{\sigma_n^2},$$

and

$$\frac{\partial^2 \log l\left(\boldsymbol{y}^{\mu}(t)|\boldsymbol{c}\right)}{\partial \beta_{\mathrm{Re}}\partial \beta_{\mathrm{Im}}} = \frac{\partial^2 \log l\left(\boldsymbol{y}^{\mu}(t)|\boldsymbol{c}\right)}{\partial \beta_{\mathrm{Im}}\partial \beta_{\mathrm{Re}}} = 0.$$

Further,

$$\frac{\partial^2 \log l\left(\boldsymbol{y}^{\mu}(t)|\boldsymbol{c}\right)}{\partial f_{\mathrm{D}_{ij}}^{\mu}\partial \beta_{\mathrm{Re}}} = -\frac{4\pi}{\sigma_n^2}\int_{-\infty}^{\infty}\left(\mathrm{Re}\left\{j y_{ij}^{\mu}(t)\left(t-\tau_{ij}^{\mu}\right) \times u_i^*\left(t-\tau_{ij}^{\mu}\right)e^{-j2\pi\left(f_{\mathrm{D}_{ij}}^{\mu}\left(t-\tau_{ij}^{\mu}\right)-f_{\mathrm{c}i}\tau_{ij}^{\mu}\right)}\right\}\right)\mathrm{d}t.$$

To compute the MFIM, we need to take the expected value of these second order derivative terms using the joint density function of the measurements and the transmitted codewords. Therefore,

$$-E\left\{\frac{\partial^2 \log l\left(\boldsymbol{y}^{\mu}(t)|\boldsymbol{c}\right)}{\partial f_{\mathrm{D}_{ij}}^{\mu}\partial \beta_{\mathrm{Re}}}\right\} = E\left\{\frac{4\pi}{\sigma_n^2}\int_{-\infty}^{\infty}\mathrm{Re}\left\{j\beta u_i\left(t-\tau_{ij}^{\mu}\right)e^{j2\pi\left(f_{\mathrm{D}_{ij}}^{\mu}\left(t-\tau_{ij}^{\mu}\right)-f_{\mathrm{c}i}\tau_{ij}^{\mu}\right)} \times (t-\tau_{ij}^{\mu})u_i^*(t-\tau_{ij}^{\mu})e^{j2\pi\left(-f_{\mathrm{D}_{ij}}^{\mu}\left(t-\tau_{ij}^{\mu}\right)+f_{\mathrm{c}i}\tau_{ij}^{\mu}\right)}\right\}\mathrm{d}t\right\},$$
$$= E\left\{\frac{4\pi}{\sigma_n^2}\int_{-\infty}^{\infty}\left(\mathrm{Re}\left\{j\beta t\left|u_i\left(t\right)\right|^2\right\}\right)\mathrm{d}t\right\},$$
$$= E\left\{\frac{4\pi}{\sigma_n^2}\int_{-\infty}^{\infty}\left(\mathrm{Re}\left\{j\beta t\sum_{n=0}^{N-1}\sum_{n'=0}^{N-1}\frac{1}{N}c_{in}g_i(t-nT) \times c_{in'}^*g_i^*(t-n'T)\right\}\right)\mathrm{d}t\right\}.$$

Since the transmitted symbols at different intervals are independent, we obtain

$$-E\left\{\frac{\partial^2 \log l\left(\boldsymbol{y}^{\mu}(t)|\boldsymbol{c}\right)}{\partial f_{\mathrm{D}_{ij}}^{\mu}\partial \beta_{\mathrm{Re}}}\right\} = \frac{4\pi}{N\sigma_n^2}\sum_{n=0}^{N-1}\int_{-\infty}^{\infty}\left(\mathrm{Re}\left\{j\beta t\left|h_i(t-nT-\frac{D}{2})\right|^2\right\}\right)\mathrm{d}t,$$
$$= \frac{4\pi}{N\sigma_n^2}\sum_{n=0}^{N-1}\int_{-\infty}^{\infty}\left(\mathrm{Re}\left\{j\beta t\left|h_i(t)\right|^2\right\}\right)\mathrm{d}t + \frac{4\pi}{N\sigma_n^2}\sum_{n=0}^{N-1}\int_{-\infty}^{\infty}\left(\mathrm{Re}\left\{j\left(nT+\frac{D}{2}\right)\beta\left|h_i(t)\right|^2\right\}\right)\mathrm{d}t.$$

From the first term, we notice that when compared to the second term, it has the variable $t$ inside the integral. Therefore, this term becomes an odd function and integrates to zero. The second term

$$\frac{4\pi}{N\sigma_n^2}\sum_{n=0}^{N-1}\int_{-\infty}^{\infty}\left(\mathrm{Re}\left\{j\left(nT+\frac{D}{2}\right)\beta\left|h_i(t)\right|^2\right\}\right)\mathrm{d}t = -\frac{4\pi\beta_{\mathrm{Im}}}{N\sigma_n^2}\sum_{n=0}^{N-1}\left(nT+\frac{D}{2}\right).$$

Hence,

$$E\left\{\frac{\partial^2 \log l\left(\boldsymbol{y}^\mu(t)|\boldsymbol{c}\right)}{\partial f^\mu_{\mathrm{D}_{ij}}\partial\beta_{\mathrm{Re}}}\right\} = \frac{4\pi\beta_{\mathrm{Im}}}{N\sigma_n^2}\sum_{n=0}^{N-1}\left(nT+\frac{D}{2}\right), \\ = \frac{4\pi\beta_{\mathrm{Im}}}{\sigma_n^2}\left(\frac{T(N-1)}{2}+\frac{D}{2}\right).$$

Next,

$$\frac{\partial^2 \log l\left(\boldsymbol{y}^\mu(t)|\boldsymbol{c}\right)}{\partial f^\mu_{\mathrm{D}_{ij}}\partial\beta_{\mathrm{Im}}} = -\frac{4\pi}{\sigma_n^2}\int_{-\infty}^{\infty}\left(\mathrm{Im}\left\{jy^\mu_{ij}(t)\left(t-\tau^\mu_{ij}\right)\right.\right. \\ \left.\left.\times\ u_i^*\left(t-\tau^\mu_{ij}\right)e^{-j2\pi\left(f^\mu_{\mathrm{D}_{ij}}\left(t-\tau^\mu_{ij}\right)-f_{\mathrm{ci}}\tau^\mu_{ij}\right)}\right\}\right)\mathrm{d}t,$$

and hence,

$$E\left\{\frac{\partial^2 \log l\left(\boldsymbol{y}^\mu(t)|\boldsymbol{c}\right)}{\partial f^\mu_{\mathrm{D}_{ij}}\partial\beta_{\mathrm{Im}}}\right\} = \\ -E\left\{\frac{4\pi}{\sigma_n^2}\int_{-\infty}^{\infty}\mathrm{Im}\left\{j\beta u_i\left(t-\tau^\mu_{ij}\right)e^{j2\pi\left(f^\mu_{\mathrm{D}_{ij}}\left(t-\tau^\mu_{ij}\right)-f_{\mathrm{ci}}\tau^\mu_{ij}\right)}\right.\right. \\ \left.\left.\times\ (t-\tau^\mu_{ij})u_i^*(t-\tau^\mu_{ij})e^{-j2\pi\left(f^\mu_{\mathrm{D}_{ij}}\left(t-\tau^\mu_{ij}\right)-f_{\mathrm{ci}}\tau^\mu_{ij}\right)}\right\}\mathrm{d}t\right\}.$$

After simplification

$$E\left\{\frac{\partial^2 \log l\left(\boldsymbol{y}^\mu(t)|\boldsymbol{c}\right)}{\partial f^\mu_{\mathrm{D}_{ij}}\partial\beta_{\mathrm{Im}}}\right\} = \\ -E\left\{\frac{4\pi}{\sigma_n^2}\int_{-\infty}^{\infty}\mathrm{Im}\left\{j\beta u_i\left(t-\tau^\mu_{ij}\right)\left(t-\tau^\mu_{ij}\right)u_i^*\left(t-\tau^\mu_{ij}\right)\right\}\mathrm{d}t\right\}.$$

Using similar process as the results above, we obtain

$$E\left\{\frac{\partial^2 \log l\left(\boldsymbol{y}^\mu(t)|\boldsymbol{c}\right)}{\partial f^\mu_{\mathrm{D}_{ij}}\partial\beta_{\mathrm{Im}}}\right\} = \\ -\frac{4\pi}{N\sigma_n^2}\mathrm{Im}\left\{j\beta\sum_{n=0}^{N-1}\int_{-\infty}^{\infty}\left(t+nT+\frac{D}{2}\right)\left|h_i(t)\right|^2\mathrm{d}t\right\}, \\ = -\frac{4\pi}{N\sigma_n^2}\mathrm{Im}\left\{j\beta\sum_{n=0}^{N-1}\left(nT+\frac{D}{2}\right)\right\}, \\ = -\frac{4\pi}{\sigma_n^2}\beta_{\mathrm{Re}}\left(\frac{T(N-1)}{2}+\frac{D}{2}\right).$$

$$\frac{\partial^2 \log l\left(\boldsymbol{y}^\mu(t)|\boldsymbol{c}\right)}{\partial \tau^\mu_{ij}\partial\beta_{\mathrm{Re}}} = \\ \frac{2}{\sigma_n^2}\int_{-\infty}^{\infty}\mathrm{Re}\left\{y^\mu_{ij}(t)\frac{\partial u_i^*\left(t-\tau^\mu_{ij}\right)}{\partial\tau^\mu_{ij}}\right. \\ \left. e^{-j2\pi\left(f^\mu_{\mathrm{D}_{ij}}\left(t-\tau^\mu_{ij}\right)-f_{\mathrm{ci}}\tau^\mu_{ij}\right)}\right\}\mathrm{d}t \\ +\frac{4\pi\left(f_{\mathrm{ci}}+f^\mu_{\mathrm{D}_{ij}}\right)}{\sigma_n^2}\int_{-\infty}^{\infty}\left(\mathrm{Re}\left\{jy^\mu_{ij}(t)u_i^*\left(t-\tau^\mu_{ij}\right)\right.\right. \\ \left.\left.\times\ e^{-j2\pi\left(f^\mu_{\mathrm{D}_{ij}}\left(t-\tau^\mu_{ij}\right)-f_{\mathrm{ci}}\tau^\mu_{ij}\right)}\right\}\right)\mathrm{d}t.$$

Therefore, taking the expected value of this expression, we get

$$E\left\{\frac{\partial^2 \log l\left(\boldsymbol{y}^\mu(t)|\boldsymbol{c}\right)}{\partial \tau^\mu_{ij}\partial\beta_{\mathrm{Re}}}\right\} = \\ \frac{2}{\sigma_n^2}E\left\{\int_{-\infty}^{\infty}\left(\mathrm{Re}\left\{\beta u_i\left(t-\tau^\mu_{ij}\right)\frac{\partial u_i^*\left(t-\tau^\mu_{ij}\right)}{\partial\tau^\mu_{ij}}\right\}\right)\mathrm{d}t\right. \\ +\frac{4\pi\left(f_{\mathrm{ci}}+f^\mu_{\mathrm{D}_{ij}}\right)}{\sigma_n^2}\int_{-\infty}^{\infty}\mathrm{Re}\left\{j\beta u_i\left(t-\tau^\mu_{ij}\right)\right. \\ \left.\left. u_i^*\left(t-\tau^\mu_{ij}\right)\right\}\mathrm{d}t\right\}.$$

It can be easily shown that this equation simplifies to

$$E\left\{\frac{\partial^2 \log l\left(\boldsymbol{y}^\mu(t)|\boldsymbol{c}\right)}{\partial \tau^\mu_{ij}\partial\beta_{\mathrm{Re}}}\right\} = \\ \frac{2}{\sigma_n^2}E\left\{\int_{-\infty}^{\infty}\left(\mathrm{Re}\left\{\beta u_i\left(t-\tau^\mu_{ij}\right)\frac{\partial u_i^*\left(t-\tau^\mu_{ij}\right)}{\partial\tau^\mu_{ij}}\right\}\right)\mathrm{d}t\right. \\ \left.-\frac{4\pi\beta_{\mathrm{Im}}\left(f_{\mathrm{ci}}+f^\mu_{\mathrm{D}_{ij}}\right)}{\sigma_n^2}\right\},$$

$$E\left\{\frac{\partial^2 \log l\left(\boldsymbol{y}^\mu(t)|\boldsymbol{c}\right)}{\partial \tau^\mu_{ij}\partial\beta_{\mathrm{Re}}}\right\} = \\ -\frac{2}{N\sigma_n^2}\int_{-\infty}^{\infty}\sum_{n=0}^{N-1}\left(\mathrm{Re}\left\{\beta h_i(t)\frac{\partial h_i^*(t)}{\partial t}\right\}\right)\mathrm{d}t \\ -\frac{4\pi\beta\mathrm{Im}\left(f_{\mathrm{ci}}+f^\mu_{\mathrm{D}_{ij}}\right)}{\sigma_n^2},.$$

The first term in the above expression is zero because the transmitted RRC pulses are even functions and the first derivatives of even functions are always odd functions, thereby forcing the value of the two sided integral to zero. Therefore,

$$E\left\{\frac{\partial^2 \log l\left(\boldsymbol{y}^\mu(t)|\boldsymbol{c}\right)}{\partial \tau^\mu_{ij}\partial\beta_{\mathrm{Re}}}\right\} = -\frac{4\pi\beta_{\mathrm{Im}}\left(f_{\mathrm{ci}}+f^\mu_{\mathrm{D}_{ij}}\right)}{\sigma_n^2}.$$

Next, we have

$$\frac{\partial^2 \log l\left(\boldsymbol{y}^\mu(t)|\boldsymbol{c}\right)}{\partial \tau^\mu_{ij}\partial\beta_{\mathrm{Im}}} = \\ \frac{2}{\sigma_n^2}\int_{-\infty}^{\infty}\mathrm{Im}\left\{y^\mu_{ij}(t)\frac{\partial u_i^*\left(t-\tau^\mu_{ij}\right)}{\partial\tau^\mu_{ij}}\right. \\ \left. e^{-j2\pi\left(f^\mu_{\mathrm{D}_{ij}}\left(t-\tau^\mu_{ij}\right)-f_{\mathrm{ci}}\tau^\mu_{ij}\right)}\right\}\mathrm{d}t \\ +\frac{4\pi\left(f_{\mathrm{ci}}+f^\mu_{\mathrm{D}_{ij}}\right)}{\sigma_n^2}\int_{-\infty}^{\infty}\left(\mathrm{Im}\left\{jy^\mu_{ij}(t)u_i^*\left(t-\tau^\mu_{ij}\right)\right.\right. \\ \left.\left.\times\ e^{-j2\pi\left(f^\mu_{\mathrm{D}_{ij}}\left(t-\tau^\mu_{ij}\right)-f_{\mathrm{ci}}\tau^\mu_{ij}\right)}\right\}\right)\mathrm{d}t.$$

Taking the expected value of this term

$$E\left\{\frac{\partial^2 \log l\left(\boldsymbol{y}^\mu(t)|\boldsymbol{c}\right)}{\partial\tau_{ij}^\mu\partial\beta_{\mathrm{Im}}}\right\} = \frac{2}{\sigma_n^2}\int_{-\infty}^{\infty} E\left\{\mathrm{Im}\left\{\beta u_i\left(t-\tau_{ij}^\mu\right)\frac{\partial u_i^*\left(t-\tau_{ij}^\mu\right)}{\partial\tau_{ij}^\mu}\right\}\mathrm{d}t + \frac{4\pi\left(f_{\mathrm{ci}}+f_{\mathrm{D}_{ij}}^\mu\right)}{\sigma_n^2}\int_{-\infty}^{\infty}\mathrm{Im}\left\{j\beta u_i\left(t-\tau_{ij}^\mu\right) u_i^*\left(t-\tau_{ij}^\mu\right)\right\}\mathrm{d}t\right\}.$$

Following the same approach as earlier, the first term of the above expression becomes zero because the term inside the integral is an odd function. Further, the waveforms from each transmitter are unit energy waveforms. Therefore, we have

$$E\left\{\frac{\partial^2 \log l\left(\boldsymbol{y}^\mu(t)|\boldsymbol{c}\right)}{\partial\tau_{ij}^\mu\partial\beta_{\mathrm{Im}}}\right\} = \frac{4\pi\beta_{\mathrm{Re}}\left(f_{\mathrm{ci}}+f_{\mathrm{D}_{ij}}^\mu\right)}{\sigma_n^2}.$$

So far, we have computed all the second order derivatives involving the attenuations variables. The second order derivatives with respect to the Doppler terms

$$\frac{\partial^2 \log l\left(\boldsymbol{y}^\mu(t)|\boldsymbol{c}\right)}{\partial {f_{\mathrm{D}_{ij}}^\mu}^2} = -\frac{8\pi^2}{\sigma_n^2}\int_{-\infty}^{\infty}\left(\mathrm{Re}\left\{\beta^* y_{ij}^\mu(t)\left(t-\tau_{ij}^\mu\right)^2 u_i^*\left(t-\tau_{ij}^\mu\right) \times e^{-j2\pi\left(f_{\mathrm{D}_{ij}}^\mu\left(t-\tau_{ij}^\mu\right)-f_{\mathrm{ci}}\tau_{ij}^\mu\right)}\right\}\right)\mathrm{d}t.$$

We compute the expected value of this term as

$$E\left\{\frac{\partial^2 \log l\left(\boldsymbol{y}^\mu(t)|\boldsymbol{c}\right)}{\partial {f_{\mathrm{D}_{ij}}^\mu}^2}\right\} = -\frac{8\pi^2}{\sigma_n^2}E\left\{\int_{-\infty}^{\infty}\left(\mathrm{Re}\left\{|\beta|^2\left(t-\tau_{ij}^\mu\right)^2 u_i\left(t-\tau_{ij}^\mu\right) \times u_i^*\left(t-\tau_{ij}^\mu\right)\right\}\right)\mathrm{d}t\right\},$$
$$= -\frac{8\pi^2}{\sigma_n^2}E\left\{\mathrm{Re}\left\{|\beta|^2\int_{-\infty}^{\infty}t^2\left|u_i(t)\right|^2\mathrm{d}t\right\}\right\},.$$

The term inside the integral in the above equation has been derived in [14] while computing the MCRLB for the passive UMTS-based monostatic radar systems.

$$E\left\{\int_{-\infty}^{\infty}t^2\left|u_i(t)\right|^2\mathrm{d}t\right\} = \frac{T^2}{16\alpha_i}+\frac{D^2}{4} + \frac{DT(N-1)}{2}+\frac{T^2(N-1)(2N-1)}{6}.$$

Substituting this result, we finally express the second-order derivatives with respect to the Doppler terms as

$$E\left\{\frac{\partial^2 \log l\left(\boldsymbol{y}^\mu(t)|\boldsymbol{c}\right)}{\partial {f_{\mathrm{D}_{ij}}^\mu}^2}\right\} = -\frac{8\pi^2|\beta|^2}{\sigma_n^2}\left(\frac{T^2}{16\alpha_i}+\frac{D^2}{4} + \frac{DT(N-1)}{2}+\frac{T^2(N-1)(2N-1)}{6}\right).$$

Note that when $i \neq i'$ and/or $j \neq j'$,

$$\frac{\partial^2 \log l\left(\boldsymbol{y}^\mu(t)|\boldsymbol{c}\right)}{\partial f_{\mathrm{D}_{ij}}^\mu\partial f_{\mathrm{D}_{i'j'}}^\mu} = 0.$$

Next, we have the second-order cross derivative terms involving both the delay and the Doppler frequency parameters

$$\begin{aligned}\frac{\partial^2 \log l\left(\boldsymbol{y}^\mu(t)|\boldsymbol{c}\right)}{\partial\tau_{ij}^\mu\partial f_{\mathrm{D}_{ij}}^\mu} = &-\frac{4\pi}{\sigma_n^2}\int_{-\infty}^{\infty}\left(\mathrm{Re}\left\{j\beta^* y_{ij}^\mu(t)\left(t-\tau_{ij}^\mu\right)\frac{\partial u_i^*\left(t-\tau_{ij}^\mu\right)}{\partial\tau_{ij}^\mu} \times e^{-j2\pi\left(f_{\mathrm{D}_{ij}}^\mu\left(t-\tau_{ij}^\mu\right)-f_{\mathrm{ci}}\tau_{ij}^\mu\right)}\right\}\right)\mathrm{d}t\\ &+\frac{4\pi}{\sigma_n^2}\int_{-\infty}^{\infty}\left(\mathrm{Re}\left\{j\beta^* y_{ij}^\mu(t)u_i^*\left(t-\tau_{ij}^\mu\right) \times e^{-j2\pi\left(f_{\mathrm{D}_{ij}}^\mu\left(t-\tau_{ij}^\mu\right)-f_{\mathrm{ci}}\tau_{ij}^\mu\right)}\right\}\right)\mathrm{d}t\\ &-\frac{8\pi^2\left(f_{\mathrm{ci}}+f_{\mathrm{D}_{ij}}^\mu\right)}{\sigma_n^2}\int_{-\infty}^{\infty}\left(\mathrm{Re}\left\{\beta^* y_{ij}^\mu(t)\left(t-\tau_{ij}^\mu\right) \times u_i^*\left(t-\tau_{ij}^\mu\right)e^{-j2\pi\left(f_{\mathrm{D}_{ij}}^\mu\left(t-\tau_{ij}^\mu\right)-f_{\mathrm{ci}}\tau_{ij}^\mu\right)}\right\}\right)\mathrm{d}t.\end{aligned}$$

Upon substituting the expressions for the expected values of the measurements, we obtain,

$$\begin{aligned}E\left\{\frac{\partial^2 \log l\left(\boldsymbol{y}^\mu(t)|\boldsymbol{c}\right)}{\partial\tau_{ij}^\mu\partial f_{\mathrm{D}_{ij}}^\mu}\right\} = &-\frac{4\pi}{\sigma_n^2}E\left\{\int_{-\infty}^{\infty}\left(\mathrm{Re}\left\{j|\beta|^2\left(t-\tau_{ij}^\mu\right)u_i\left(t-\tau_{ij}^\mu\right) \times \frac{\partial u_i^*\left(t-\tau_{ij}^\mu\right)}{\partial\tau_{ij}^\mu}\right\}\right)\mathrm{d}t\right.\\ &+\frac{4\pi}{\sigma_n^2}\int_{-\infty}^{\infty}\left(\mathrm{Re}\left\{j|\beta|^2 u_i\left(t-\tau_{ij}^\mu\right)u_i^*\left(t-\tau_{ij}^\mu\right)\right\}\right)\mathrm{d}t\\ &\left.-\frac{8\pi^2\left(f_{\mathrm{ci}}+f_{\mathrm{D}_{ij}}^\mu\right)}{\sigma_n^2}\int_{-\infty}^{\infty}\left(\mathrm{Re}\left\{|\beta|^2\left(t-\tau_{ij}^\mu\right) \times u_i\left(t-\tau_{ij}^\mu\right)u_i^*\left(t-\tau_{ij}^\mu\right)\right\}\right)\mathrm{d}t\right\}.\end{aligned}$$

We can simplify the above expression to

$$E\left\{\frac{\partial^2 \log l\left(\boldsymbol{y}^{\mu}(t)|\boldsymbol{c}\right)}{\partial\tau_{ij}^{\mu}\partial f_{\mathrm{D}_{ij}}^{\mu}}\right\}=$$
$$\frac{4\pi}{N\sigma_n^2}\int_{-\infty}^{\infty}\sum_{n=0}^{N-1}\left(\mathrm{Re}\left\{j\left|\beta\right|^2\left(t+nT+\frac{D}{2}\right)\right.\right.$$
$$\left.\left.\times\; h_i\left(t\right)\frac{\partial h_i^*\left(t\right)}{\partial t}\right\}\right)\mathrm{d}t$$
$$+\frac{4\pi}{N\sigma_n^2}\int_{-\infty}^{\infty}\sum_{n=0}^{N-1}\left(\mathrm{Re}\left\{j\left|\beta\right|^2 h_i\left(t\right)h_i^*\left(t\right)\right\}\right)\mathrm{d}t$$
$$-\frac{8\pi^2\left(f_{\mathrm{ci}}+f_{\mathrm{D}_{ij}}^{\mu}\right)}{N\sigma_n^2}\int_{-\infty}^{\infty}\sum_{n=0}^{N-1}\left(\mathrm{Re}\left\{\left|\beta\right|^2\left(t+nT+\frac{D}{2}\right)\right.\right.$$
$$\left.\left.\times\; h_i\left(t\right)h_i^*\left(t\right)\right\}\right)\mathrm{d}t.$$

This further simplifies to

$$E\left\{\frac{\partial^2 \log l\left(\boldsymbol{y}^{\mu}(t)|\boldsymbol{c}\right)}{\partial\tau_{ij}^{\mu}\partial f_{\mathrm{D}_{ij}}^{\mu}}\right\}=$$
$$\frac{4\pi}{N\sigma_n^2}\sum_{n=0}^{N-1}\left(\mathrm{Re}\left\{j\left|\beta\right|^2\int_{-\infty}^{\infty}t h_i\left(t\right)\frac{\partial h_i^*\left(t\right)}{\partial t}\mathrm{d}t\right\}\right)$$
$$+\frac{4\pi}{N\sigma_n^2}\sum_{n=0}^{N-1}\mathrm{Re}\left\{j\left|\beta\right|^2\int_{-\infty}^{\infty}h_i\left(t\right)h_i^*\left(t\right)\mathrm{d}t\right\}$$
$$-\frac{8\pi^2\left(f_{\mathrm{ci}}+f_{\mathrm{D}_{ij}}^{\mu}\right)}{N\sigma_n^2}\sum_{n=0}^{N-1}\left(\mathrm{Re}\left\{\left|\beta\right|^2\left(nT+\frac{D}{2}\right)\right.\right.$$
$$\left.\left.\times\int_{-\infty}^{\infty}h_i\left(t\right)h_i^*\left(t\right)\mathrm{d}t\right\}\right).$$

Note that we used the fact that the first derivative of the RRC waveform is an odd function. Further, for the term, the expression inside the integral is purely imaginary because the RRC waveform is real. Therefore,

$$E\left\{\frac{\partial^2 \log l\left(\boldsymbol{y}^{\mu}(t)|\boldsymbol{c}\right)}{\partial\tau_{ij}^{\mu}\partial f_{\mathrm{D}_{ij}}^{\mu}}\right\}=$$
$$-\frac{8\pi^2|\beta|^2\left(f_{\mathrm{ci}}-f_{\mathrm{D}_{ij}}^{\mu}\right)}{N\sigma_n^2}\sum_{n=0}^{N-1}\left(nT+\frac{D}{2}\right),$$
$$=-\frac{8\pi^2|\beta|^2\left(f_{\mathrm{ci}}+f_{\mathrm{D}_{ij}}^{\mu}\right)}{\sigma_n^2}\left(\frac{T(N-1)}{2}+\frac{D}{2}\right).$$

The final term remaining in the second order derivatives

$$\frac{\partial^2 \log l\left(\boldsymbol{y}^{\mu}(t)|\boldsymbol{c}\right)}{\partial{\tau_{ij}^{\mu}}^2}=$$
$$\frac{2}{\sigma_n^2}\int_{-\infty}^{\infty}\left(\mathrm{Re}\left\{\beta^* y_{ij}^{\mu}(t)\frac{\partial^2 u_i^*\left(t-\tau_{ij}^{\mu}\right)}{\partial{\tau_{ij}^{\mu}}^2}\right.\right.$$
$$\left.\left.\times\; e^{-j2\pi\left(f_{\mathrm{D}_{ij}}^{\mu}\left(t-\tau_{ij}^{\mu}\right)-f_{\mathrm{ci}}\tau_{ij}^{\mu}\right)}\right\}\right)\mathrm{d}t$$
$$+\frac{8\pi\left(f_{\mathrm{ci}}+f_{\mathrm{D}_{ij}}^{\mu}\right)}{\sigma_n^2}\int_{-\infty}^{\infty}\left(\mathrm{Re}\left\{j\beta^* y_{ij}^{\mu}(t)\frac{\partial u_i^*\left(t-\tau_{ij}^{\mu}\right)}{\partial\tau_{ij}^{\mu}}\right.\right.$$
$$\left.\left.\times\; e^{-j2\pi\left(f_{\mathrm{D}_{ij}}^{\mu}\left(t-\tau_{ij}^{\mu}\right)-f_{\mathrm{ci}}\tau_{ij}^{\mu}\right)}\right\}\right)\mathrm{d}t$$
$$+-\frac{8\pi^2\left(f_{\mathrm{ci}}+f_{\mathrm{D}_{ij}}^{\mu}\right)^2}{\sigma_n^2}\int_{-\infty}^{\infty}\left(\mathrm{Re}\left\{\beta^* y_{ij}^{\mu}(t)u_i^*\left(t-\tau_{ij}^{\mu}\right)\right.\right.$$
$$\left.\left.\times\; e^{-j2\pi\left(f_{\mathrm{D}_{ij}}^{\mu}\left(t-\tau_{ij}^{\mu}\right)-f_{\mathrm{ci}}\tau_{ij}^{\mu}\right)}\right\}\right)\mathrm{d}t.$$

The expected value

$$E\left\{\frac{\partial^2 \log l\left(\boldsymbol{y}^{\mu}(t)|\boldsymbol{c}\right)}{\partial{\tau_{ij}^{\mu}}^2}\right\}=$$
$$\frac{2}{\sigma_n^2}E\left\{\int_{-\infty}^{\infty}\mathrm{Re}\left\{\left|\beta\right|^2 u_i\left(t-\tau_{ij}^{\mu}\right)\frac{\partial^2 u_i^*\left(t-\tau_{ij}^{\mu}\right)}{\partial{\tau_{ij}^{\mu}}^2}\right\}\mathrm{d}t\right.$$
$$+\frac{8\pi\left(f_{\mathrm{ci}}+f_{\mathrm{D}_{ij}}^{\mu}\right)}{\sigma_n^2}\int_{-\infty}^{\infty}\left(\mathrm{Re}\left\{j\left|\beta\right|^2 u_i\left(t-\tau_{ij}^{\mu}\right)\right.\right.$$
$$\left.\left.\times\frac{\partial u_i^*\left(t-\tau_{ij}^{\mu}\right)}{\partial\tau_{ij}^{\mu}}\right\}\right)\mathrm{d}t$$
$$+-\frac{8\pi^2\left(f_{\mathrm{ci}}+f_{\mathrm{D}_{ij}}^{\mu}\right)^2}{\sigma_n^2}\int_{-\infty}^{\infty}\left(\mathrm{Re}\left\{\left|\beta\right|^2 u_i\left(t-\tau_{ij}^{\mu}\right)\right.\right.$$
$$\left.\left.\left.\times u_i^*\left(t-\tau_{ij}^{\mu}\right)\right\}\right)\mathrm{d}t\right\}.$$

The second term in the above expression contains an odd function in the integral. Therefore,

$$E\left\{\frac{\partial^2 \log l\left(\boldsymbol{y}^{\mu}(t)|\boldsymbol{c}\right)}{\partial{\tau_{ij}^{\mu}}^2}\right\}=$$
$$\frac{2\left|\beta\right|^2}{\sigma_n^2}E\left\{\int_{-\infty}^{\infty}\left(h_i\left(t\right)\frac{\partial^2 h_i^*\left(t\right)}{\partial t^2}\right)\mathrm{d}t\right\}$$
$$-\frac{8\pi^2\left|\beta\right|^2\left(f_{\mathrm{ci}}+f_{\mathrm{D}_{ij}}^{\mu}\right)^2}{\sigma_n^2}.$$

For the first term, using Cauchy-Schwarz inequality,

$$\left|\int_{-\infty}^{\infty}h_i\left(t\right)\frac{\partial^2 h_i^*\left(t\right)}{\partial t^2}\mathrm{d}t\right|^2$$
$$\leq\int_{-\infty}^{\infty}\left|h_i\left(t\right)\right|^2\mathrm{d}t\int_{-\infty}^{\infty}\left|\frac{\partial^2 h_i^*\left(t\right)}{\partial t^2}\right|^2\mathrm{d}t,$$
$$\leq\int_{-\infty}^{\infty}\left|\omega^2 H_i(\omega)\right|^2\mathrm{d}\omega,$$
$$\leq 2\int_{0}^{\frac{1+\alpha_i}{2T}}\omega^4\left|H_i(\omega)\right|^2\mathrm{d}\omega,$$
$$\leq\left(\frac{1+\alpha_i}{T}\right)^2\frac{1}{12T^2}\left(1+3\alpha_i^2-24\frac{\alpha_i^2}{\pi^2}\right),$$

where $H_i(\omega)$ denotes the Fourier transform of $h_i(t)$. Here, we used the result in equation $(53)$ of [14] for obtaining the last step. Clearly, we observe that $\left|\int_{-\infty}^{\infty} h_i\,(t)\,\frac{\partial^2 h_i^*(t)}{\partial t^2}\mathrm{d}t\right|$ is of the order of $T^{-2}$. This is much smaller than $\left(f_{\mathrm{ci}} + f_{\mathrm{D}_{ij}}^{\mu}\right)^2$. Therefore, we obtain

$$E\left\{\frac{\partial^2 \log l\,(\boldsymbol{y}^{\mu}(t)|\boldsymbol{c})}{\partial \tau_{ij}^{\mu\,2}}\right\} \approx -\frac{8\pi^2\,|\beta|^2\left(f_{\mathrm{ci}} + f_{\mathrm{D}_{ij}}^{\mu}\right)^2}{\sigma_n^2}.$$

When $i \neq i'$ and/or $j \neq j'$, $\frac{\partial^2 \log l(\boldsymbol{y}^{\mu}(t)|\boldsymbol{c})}{\partial \tau_{ij}^{\mu\,2}} = 0$.

## REFERENCES


[1] H. D. Griffiths and N. R. W. Long, "Television based bistatic radar," *Proc. Inst. Electr. Eng. F—Commun. Radar Signal Process.*, vol. 133, pp. 649–657, 1986.

[2] H. A. Harms, L. M. Davis, and J. Palmer, "Understanding the signal structure in DVB-T signals for passive radar detection," presented at the IEEE Int. Radar Conf., Washington, DC, USA, May 2010.

[3] A. D. Lallo, A. Farina, R. Fulcoli, P. Genovesi, R. Lalli, and R. Mancinelli, "Design, development and test on real data of an FM based prototypical passive radar," presented at the IEEE Radar Conf., Rome, Italy, May 2008.

[4] D. Poullin, "Passive detection using digitial broadcasters (DAB,DVB) with COFDM modulation," *Proc. Inst. Electr. Eng.—Radar Sonar Navig.*, vol. 152, pp. 143–152, Jun. 2005.

[5] H. D. Griffiths and C. J. Baker, "Measurement and analysis of ambiguity functions of passive radar transmissions," presented at the IEEE Int. Radar Conf., Washington, DC, USA, May 2005.

[6] H. D. Griffiths and C. J. Baker, "Passive coherent location radar systems. Part 1: Performance prediction," in *Proc. Inst. Electr. Eng.—Radar, Sonar, Navigat.*, Jun. 2005, vol. 152, pp. 153–159.

[7] M. Malanowski and K. Kulpa, "Digital beamforming for passive coherent location radar," presented at the Radar Conf., Rome, Italy, May 2008.

[8] M. Malanowski, "Detection and parameter estimation of manoeuvring targets with passive bistatic radar," *IET Radar Sonar Navig.*, vol. 6, pp. 739–745, Oct. 2012.

[9] D. E. Hack, L. K. Patton, A. D. Kerrick, and M. A. Saville, "Direct Cartesian detection, localization, and de-ghosting for passive multistatic radar," presented at the 7th IEEE Sens. Array Multichannel Signal Process. Workshop, Hoboken, NJ, USA, Jun. 2012.

[10] J. Li and P. Stoica*, MIMO Radar Signal Processing*. Hoboken, NJ, USA: Wiley, 2009.

[11] A. M. Haimovich, R. S. Blum, and L. J. Cimini, "MIMO radar with widely separated antennas," *IEEE Signal Process. Mag.*, vol. 25, pp. 116–129, 2008.

[12] A. D. Maio and M. Lops, "Design principles of MIMO radar detectors," *IEEE Trans. Aerosp. Electron. Syst.*, vol. 43, pp. 886–898, Jul. 2007.

[13] S. Gogineni and A. Nehorai, "Target estimation using sparse modeling for distributed MIMO radar," *IEEE Trans. Signal Process.*, vol. 59, pp. 5315–5325, Nov. 2011.

[14] P. Stinco, M. S. Greco, F. Gini, and M. Rangaswamy, "Ambiguity function and Cramer-Rao bounds for universal mobile telecommunications system-based passive coherent location systems," *IET Radar Sonar Navig.*, vol. 6, pp. 668–678, Aug. 2012.

[15] P. Stoica and A. Nehorai, "MUSIC, maximum likelihood and Cramer-Rao bound," *IEEE Trans. Acoust., Speech, Signal Process.*, vol. 37, pp. 720–741, May 1989.

[16] L. L. Scharf*, Statistical Signal Processing: Detection, Estimation, and Time Series Analysis Reading*. Norwood, MA, USA: Addison-Wesley, 1991.

[17] S. Kay*, Fundamentals of Statistical Signal Processing, Volume I: Estimation Theory*. Englewood Cliffs, NJ, USA: Prentice-Hall, 1993.

[18] A. N. D'Andrea, U. Mengali, and R. Reggiannini, "The modified Cramer-Rao bound and its application to synchronization problems," *IEEE Trans. Commun.*, vol. 42, pp. 1391–1399, Feb./Mar./Apr. 1994.

[19] F. Gini, "A radar application of a modified Cramer-Rao bound: parameter estimation in non-Gaussian clutter," *IEEE Trans. Signal Process.*, vol. 46, pp. 1945–1953, Jul. 1998.

[20] F. Gini, M. Montanari, and L. Verrazzani, "Estimation of chirp radar signals in compound-Gaussian clutter: a cyclostationary approach," *IEEE Trans. Signal Process.*, vol. 48, pp. 1029–1039, Apr. 2000.

[21] Q. He, R. S. Blum, and A. M. Haimovich, "Non-coherent MIMO radar for target estimation: More antennas means better performance," in *Proc. 43rd Annu. Conf. Inf. Sci. Syst.*, Baltimore, MD, USA, Mar. 2009.

[22] T. Tsao, M. Slamani, P. Varshney, and D. Weiner, "Ambiguity function for a bistatic radar," *IEEE Trans. Aerosp. Electron. Syst.*, vol. 33, pp. 1041–1051, 1997.

[23] A. Dogandzic and A. Nehorai, "Cramer-Rao bounds for estimating range, velocity, and direction with an active sensor array," *IEEE Trans. Signal Process.*, vol. 49, pp. 1122–1138, Jun. 2001.

[24] C. Wei, Q. He, and R. S. Blum, "Cramer-Rao bound for joint location and velocity estimation in multi-target non-coherent MIMO radars," presented at the 44th Ann. Conf. Inf. Sci. Syst., Princeton, NJ, USA, Mar. 2010.

[25] H. Godrich, A. M. Haimovich, and R. S. Blum, "Cramer Rao bound on target localization estimation in MIMO radar systems," in *Proc. 42nd Annu. Conf. Inf. Sci. Syst.*, Princeton, NJ, USA, Mar. 2008, pp. 134–139.

[26] M. Jin, G. Liao, and J. Li, "Target localisation for distributed multiple-input multiple-output radar and its performance analysis," *IET Radar, Sonar Navig.*, vol. 5, pp. 83–91, Jan. 2011.

[27] H. Godrich, A. M. Haimovich, and R. S. Blum, "Target localization accuracy gain in MIMO radar-based systems," *IEEE Trans. Inf. Theory*, vol. 56, pp. 2783–2803, 2010.

[28] Q. He and R. S. Blum, "Noncoherent versus coherent MIMO radar: Performance and simplicity analysis, signal processing," *Signal Process.*, vol. 92, pp. 2454–2463, Oct. 2012.

[29] M. Akcakaya and A. Nehorai, "MIMO radar detection and adaptive design under a phase synchronization mismatch," *IEEE Trans. Signal Process.*, vol. 58, pp. 4994–5005, Oct. 2010.

[30] A. Fletcher and F. Robey, "11th conf. adaptive sensors array processing," presented at the Proc. 3rd Eur. Radar Conf., Lexington, MA, USA, Mar. 2003.

[31] I. Papoutsis, C. Baker, and H. Griffiths, "Fundamental performance limitations of radar networks," presented at the 1st EMRS DTC Tech. Conf., Edinburgh, U.K., 2004.



**Sandeep Gogineni** (S'08–M'13) received the B.Tech. degree in electronics and communications engineering (with Honors in signal processing and communications) from the International Institute of Information Technology, Hyderabad, India, in 2007. He received the M.S. and Ph.D. degrees in electrical engineering from Washington University, St. Louis, MO, in 2009 and 2012, respectively.

He is a Research Engineer at Wright State Research Institute, Dayton, OH. His research interests are in statistical signal processing, radar and communications systems.

Dr. Gogineni won the Best Paper Award (First Prize) in the Student Paper Competition at the 2012 International Waveform Diversity and Design (WDD) Conference. Further, he was selected as a Finalist in the Student Paper Competitions at the 2010 International Waveform Diversity and Design (WDD) Conference and 2011 IEEE Digital Signal Processing and Signal Processing Education Workshop.

**Muralidhar Rangaswamy** (S'89–M'93–SM'98–F'06) received the B.E. degree in electronics engineering from Bangalore University, Bangalore, India, in 1985 and the M.S. and Ph.D. degrees in electrical engineering from Syracuse University, Syracuse, NY, in 1992.

He is a Senior Advisor for Radar Research at the RF Exploitation Branch within the Sensors Directorate of the Air Force Research Laboratory (AFRL). Prior to this, he held industrial and academic appointments. His research interests include radar signal processing, spectrum estimation, modeling non-Gaussian interference phenomena, and statistical communication theory. He has coauthored more than 150 refereed journal and conference record papers in the areas of his research interests. Additionally, he is a contributor to 8 books and is a co-inventor on 3 U.S. patents.

Dr. Rangaswamy is the Technical Editor (Associate Editor-in-Chief) for Radar Systems in the IEEE TRANSACTIONS ON AEROSPACE AND ELECTRONIC SYSTEMS (IEEE-TAES). He served as the Co-Editor-in-Chief for the *Digital Signal Processing* journal between 2005 and 2011. He serves on the Senior Editorial Board of the IEEE JOURNAL OF SELECTED TOPICS IN SIGNAL PROCESSING (Jan. 2012-Dec. 2014). He was a 2–term elected member of the sensor array and multichannel processing technical committee (SAM-TC) of the IEEE Signal Processing Society between January 2005 and December 2010 and serves as a member of the Radar Systems Panel (RSP) in the IEEE-AES Society. He was the General Chairman for the 4th IEEE Workshop on Sensor Array and Multichannel Processing (SAM-2006), Waltham, MA, July 2006. He served on the Technical Committee of the IEEE Radar Conference series in a myriad of roles (Track Chair, Session Chair, Special Session Organizer and Chair, Paper Selection Committee Member, Tutorial Lecturer). He served as the Publicity Chair for the First IEEE International Conference on Waveform Diversity and Design, Edinburgh, U.K. November 2004. He presently serves on the conference subcommittee of the RSP. He is the Technical Program Chairman for the 2014 IEEE Radar Conference. He received the 2012 IEEE Warren White Radar Award, the 2013 Affiliate Societies Council Dayton (ASC-D) Outstanding Scientist and Engineer Award, the 2007 IEEE Region 1 Award, the 2006 IEEE Boston Section Distinguished Member Award, and the 2005 IEEE-AESS Fred Nathanson memorial outstanding young radar engineer award. He was elected as a Fellow of the IEEE in January 2006 with the citation "for contributions to mathematical techniques for radar space-time adaptive processing." He received the 2012 and 2005 Charles Ryan basic research award from the Sensors Directorate of AFRL, in addition to more than 40 scientific achievement awards.

**Brian D. Rigling** (S'00–M'03–SM'08) received the B.S. degree in physics-computer science from the University of Dayton in 1998 and received the M.S. and Ph.D. degrees in electrical engineering from The Ohio State University in 2000 and 2003, respectively.

From 2000 to 2004 he was a radar systems engineer for Northrop Grumman Electronic Systems in Baltimore, MD. Since July 2004, he has been with the Department of Electrical Engineering, Wright State University, and was promoted to Associate Professor in 2009 and Professor in 2013. For 2010, he was with the Science Applications International Corporation as a Chief Scientist while on leave from Wright State University.

Dr. Rigling has served on the IEEE Radar Systems Panel since 2009, and has been an Associate Editor for the IEEE TRANSACTIONS ON IMAGE PROCESSING. He is the General Chair for the 2014 IEEE Radar Conference.

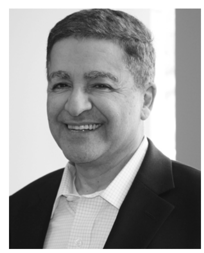

**Arye Nehorai** (S'80–M'83–SM'90–F'94) received the B.Sc. and M.Sc. degrees from the Technion, Israel, and the Ph.D. from Stanford University, CA.

He is the Eugene and Martha Lohman Professor and Chair of the Preston M. Green Department of Electrical and Systems Engineering (ESE) at Washington University, St. Louis (WUSTL). Under his leadership as department chair, the undergraduate enrollment has more than tripled in the last four years. He is also Professor in the Division of Biology and Biomedical Studies (DBBS) and Director of the Center for Sensor Signal and Information Processing at WUSTL. Earlier, he was a faculty member at Yale University and the University of Illinois at Chicago.

Dr. Nehorai served as Editor-in-Chief of the IEEE TRANSACTIONS ON SIGNAL PROCESSING from 2000 to 2002. From 2003 to 2005 he was the Vice President (Publications) of the IEEE Signal Processing Society (SPS), the Chair of the Publications Board, and a member of the Executive Committee of this Society. He was the founding editor of the special columns on Leadership Reflections in IEEE SIGNAL PROCESSING MAGAZINE from 2003 to 2006. He received the 2006 IEEE SPS Technical Achievement Award and the 2010 IEEE SPS Meritorious Service Award. He was elected Distinguished Lecturer of the IEEE SPS for a term lasting from 2004 to 2005. He received best paper awards in IEEE journals and conferences. In 2001 he was named University Scholar of the University of Illinois. He was the Principal Investigator of the Multidisciplinary University Research Initiative (MURI) project titled Adaptive Waveform Diversity for Full Spectral Dominance from 2005 to 2010. He is a Fellow of the Royal Statistical Society since 1996 and a Fellow of AAAS since 2012.